Astron. Astrophys. 350, 334–343 (1999)

ASTRONOMY AND ASTROPHYSICS

On the pair electromagnetic pulse of a black hole with electromagnetic structure

R. Ruffini[1], **J.D. Salmonson**[2], **J.R. Wilson**[2], **and S.-S. Xue**[1]

[1] I.C.R.A.-International Center for Relativistic Astrophysics and Physics Department, University of Rome "La Sapienza", I-00185 Rome, Italy
[2] Lawrence Livemore National Laboratory, University of California, Livermore, CA, USA

Received 17 March 1999 / Accepted 12 July 1999

Abstract. We study the relativistically expanding electron-positron pair plasma formed by the process of vacuum polarization around an electromagnetic black hole (EMBH). Such processes can occur for EMBH's with mass all the way up to $6 \cdot 10^5 M_\odot$. Beginning with a idealized model of a Reissner-Nordstrom EMBH with charge to mass ratio $\xi = 0.1$, numerical hydrodynamic calculations are made to model the expansion of the pair-electromagnetic pulse (PEM pulse) to the point that the system is transparent to photons. Three idealized special relativistic models have been compared and contrasted with the results of the numerically integrated general relativistic hydrodynamic equations. One of the three models has been validated: a PEM pulse of constant thickness in the laboratory frame is shown to be in excellent agreement with results of the general relativistic hydrodynamic code. It is remarkable that this precise model, starting from the fundamental parameters of the EMBH, leads uniquely to the explicit evaluation of the parameters of the PEM pulse, including the energy spectrum and the astrophysically unprecedented large Lorentz factors (up to $6 \cdot 10^3$ for a $10^3 M_\odot$ EMBH). The observed photon energy at the peak of the photon spectrum at the moment of photon decoupling is shown to range from 0.1 MeV to 4 MeV as a function of the EMBH mass. Correspondingly the total energy in photons is in the range of 10^{52} to 10^{54} ergs, consistent with observed gamma-ray bursts. In these computations we neglect the presence of baryonic matter which will be the subject of forthcoming publications.

Key words: black hole physics – gamma rays: theory – gamma rays: bursts – gamma rays: observations

1. Introduction

At present there is a need for viable source models capable of producing the large energy ($\sim 10^{53}$–10^{54} ergs) necessary to power distant gamma-ray bursts such as GRB971214 (e.g. Frontera & Piro 1999 and references therein) and GRB990123 (Bloom et al. 1999). In this paper we present a model for the production of such large bursts based on results of calculations of the energy emission from vacuum polarization processes around an EMBH.

Damour & Ruffini (1975) indicated a very precise mechanism to explain the origin of gamma ray bursts: the vacuum polarization of a Kerr-Newman EMBH via the Heisenberg-Euler-Schwinger process. They showed how these processes, occurring for EMBH's all the way up to $6 \cdot 10^5 M_\odot$, can radiate a large fraction of the extractable energy of the EMBH, in the sense of the Black Holes reversible transformations (Christodoulou & Ruffini 1971). Recently, after the discovery of the gamma ray afterglow by the Beppo Sax satellite and their optical identification (e.g. Frontera & Piro 1999), this model has been reconsidered by Ruffini (1998) who introduced the new concept of the "dyadosphere" of an EMBH and by Preparata et al. (1998a, 1998b) who have given details of the spatial density and energy distribution in the electron-positron plasma created in the dyadosphere. The present paper examines the time evolution of such an electron-positron plasma by assuming an EMBH in vacuum and calculates the consequences.

Past work on black hole formation by Wilson (1975, 1977) has shown that highly charged EMBH's with charge to mass ratio $\xi = Q/(M\sqrt{G}) \approx 0.1$, surrounded by an oppositely charged magnetosphere, may form during the collapse of rotating magnetized stars. For a low mass star to collapse and form a highly charged black hole, surrounded by an oppositely charged magnetosphere, strong initial fields and rapid rotation are required. The theoretical background for such an analysis has been presented in Ruffini & Wilson (1975), and Damour et al. (1978). The recent discovery of the soft gamma-ray repeater SGR1806-20 (Kouveliotou et al. 1998, Baring & Harding 1998) indicates that very high magnetic fields may be present in precollapse stars of a few solar masses.

The calculations by Wilson assumed space was filled with a perfect conductor so that the magneto-hydrodynamic model could be used. In the region above a newly formed EMBH the density is falling rapidly. Eventually, due to the paucity of charge carriers, the assumption of the plasma as a perfect conductor must fail, possibly leading to regions where the electric fields will be sufficiently high so that pair creation will ensue. Similar scenarios can be envisaged for gravitational collapse of much larger masses $M \sim 10^4$–$10^5 M_\odot$ occurring in galactic nuclei. In the present paper we begin with the idealized situation of an isolated, Reissner-Nordstrom EMBH with charge to mass ratio $\xi = 0.1$. The case of a Ker Newmann EMBH is presented in

Damour & Ruffini, 1999 (paper in preparation). The vacuum polarization processes are computed, following the approach outlined in Ruffini (1998), Preparata et al. (1998a, 1998b), Ruffini (1999a, 1999b), and they give the specific initial data of the dyadosphere. The evolution of the PEM pulse formed by the vacuum polarization processes is followed by a numerical calculation to the point where the system is transparent to photons. We then analyze the final gamma-ray signal that would be observed from this idealized model of an EMBH in vacuum. Extensions of this model such as the expansion of the PEM pulse in the presence of the remnant baryonic matter left over in the collapse process will be the subject of a forthcoming publication (Ruffini et al., 1999b, paper in preparation).. Some consequences for the interpretation of the observed burst and afterglow are presented in Preparata & Ruffini, 1999 and Preparata et al., 1999 (papers in preparation).

2. Formation of e^+e^- pairs from an EMBH

We recall the relevant formulas from Ruffini (1998) and Preparata et al. (1998a, 1998b):

The Christodoulou-Ruffini mass formula for a Reissner-Nordstrom black hole gives (Christodoulou & Ruffini 1971)

$$E = Mc^2 = M_{\rm ir}c^2 + \frac{Q^2}{2r_+}, \tag{1}$$

$$S = 4\pi r_+^2 = 16\pi\left(\frac{G^2}{c^4}\right)M_{\rm ir}^2, \tag{2}$$

with

$$\frac{\sqrt{G}Q}{r_+c^2} \leq 1, \tag{3}$$

where $M_{\rm ir}$ is the irreducible mass, $r_+ = 2M_{\rm ir}$ is the horizon radius, S is the horizon surface area, and maximally charged ($Q_{\rm max} = 2\sqrt{G}M_{ir}$) black holes satisfy the equality in Eq. (3).

The dyadosphere is defined as the region outside the horizon of a EMBH where the electric field exceeds the critical value for spontaneous e^+e^- pair creation, $\mathcal{E}_{\rm c} = \frac{m^2c^3}{\hbar e}$ (Heisenberg & Euler 1931, Schwinger 1951), where m and e are the mass and charge of the electron. By introducing the dimensionless mass and charge parameters $\mu = \frac{M}{M_\odot}, \xi = \frac{Q}{Q_{\rm max}} \leq 1$ for Reissner-Nordstrom black holes, the horizon radius may be expressed as

$$r_+ = \frac{GM}{c^2}\left[1+\sqrt{1-\frac{Q^2}{GM^2}}\right] = 1.47\times10^5\mu(1+\sqrt{1-\xi^2})\ {\rm cm}. \tag{4}$$

The outer limit of the dyadosphere is defined as the radius $r_{\rm ds}$ at which the electric field produced by the EMBH equals the critical field. The radius of the dyadosphere can be expressed in terms of the Planck charge $q_{\rm p} = (\hbar c)^{\frac{1}{2}}$ and the Planck mass $m_{\rm p} = (\frac{\hbar c}{G})^{\frac{1}{2}}$ in the form

$$r_{\rm ds} = \left(\frac{\hbar}{mc}\right)^{\frac{1}{2}}\left(\frac{GM}{c^2}\right)^{\frac{1}{2}}\left(\frac{m_{\rm p}}{m}\right)^{\frac{1}{2}}\left(\frac{e}{q_{\rm p}}\right)^{\frac{1}{2}}\left(\frac{Q}{\sqrt{G}M}\right)^{\frac{1}{2}} = 1.12\cdot10^8\sqrt{\mu\xi}\ {\rm cm}, \tag{5}$$

which well illustrates the hybrid gravitational and quantum nature of this quantity. The radial interval $r_+ \leq r \leq r_{\rm ds}$ describes the region in which e^+e^- pairs are produced (see Fig. 1 of Preparata et al. 1998a).

In a very short time $\sim O(\frac{\hbar}{mc^2})$, a very large number of pairs is created in the dyadosphere. The local number density of pairs created is computed as a function of radius

$$n_{e^+e^-}(r) = \frac{Q}{4\pi r^2\left(\frac{\hbar}{mc}\right)e}\left[1-\left(\frac{r}{r_{ds}}\right)^2\right], \tag{6}$$

and the energy density is given by

$$\epsilon(r) = \frac{Q^2}{8\pi r^4}\left(1-\left(\frac{r}{r_{ds}}\right)^4\right), \tag{7}$$

(see Figs. [2] & [3] of Preparata et al. 1998a). The total energy of pairs converted from the static electric energy and deposited within the dyadosphere is then

$$E^{\rm tot}_{e^+e^-} = \frac{1}{2}\frac{Q^2}{r_+}(1-\frac{r_+}{r_{\rm ds}})\left[1-\left(\frac{r_+}{r_{\rm ds}}\right)^2\right]. \tag{8}$$

In the limit of $\frac{r_+}{r_{ds}} \to 0$, Eq. (8) leads to $E^{\rm tot}_{e^+e^-} \to \frac{1}{2}\frac{Q^2}{r_+}$, which coincides with the energy extractable from EMBH's by reversible processes ($M_{ir} = {\rm const.}$), namely $E - M_{ir} = \frac{1}{2}\frac{Q^2}{r_+}$(see Fig. 4 of Preparata et al. 1998a).

Due to the very large pair density given by Eq. (6) and to the sizes of the cross-sections for the process $e^+e^- \leftrightarrow \gamma+\gamma$, the system is expected to thermalize to a plasma configuration for which

$$N_{e^+} = N_{e^-} = N_\gamma = N_{\rm p} \tag{9}$$

and reach an average temperature

$$kT_\circ = \frac{E^{\rm tot}_{e^+e^-}}{3N_{\rm p}\cdot 2.7}, \tag{10}$$

where $N_p = N_{\rm pair}$ is the number of e^+e^--pairs created in the dyadosphere and k is Boltzmann's constant (see Fig. 4 of Preparata et al. 1998b).

In conclusion, we stress that (i) the locality of e^+e^- pair creation is an important feature of the dyadosphere, and (ii) e^+e^- pair creation occurs only in a finite range of the parameters μ and ξ and a unique spectrum of the created pairs can be calculated in terms of these two parameters μ, ξ (iii) Eqs. (1-8) show that the pair-creation process is capable of extracting large amounts of energy from an EMBH with an extremely high efficiency (close to 100%).

In Wilson (1975, 1977) a black hole charge of the order $Q = 0.1Q_{\rm max}(\xi = 0.1)$ was formed. Thus, we henceforth assume an EMBH with $\xi = 0.1$ for our detailed numerical calculations. In Fig. 1 a plot of the total energy Eq. (8) versus mass is given for the case $\xi = 0.1$ and in Fig. 2 a plot of the average energy per pair (relating to Eq. (10)) versus mass is given also for $\xi = 0.1$.

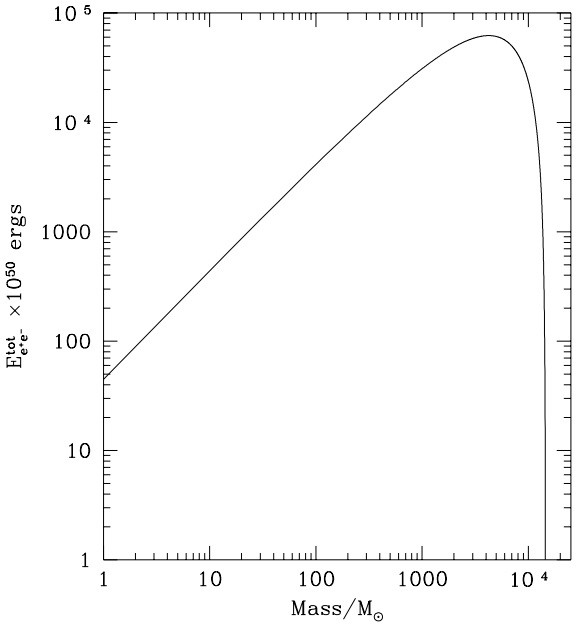

Fig. 1. The total energy in e^+e^- pairs deposited within the dyadosphere of a black hole with mass M and charge $Q = 0.1Q_{\rm max}$ equal to 10% of maximal black hole charge.

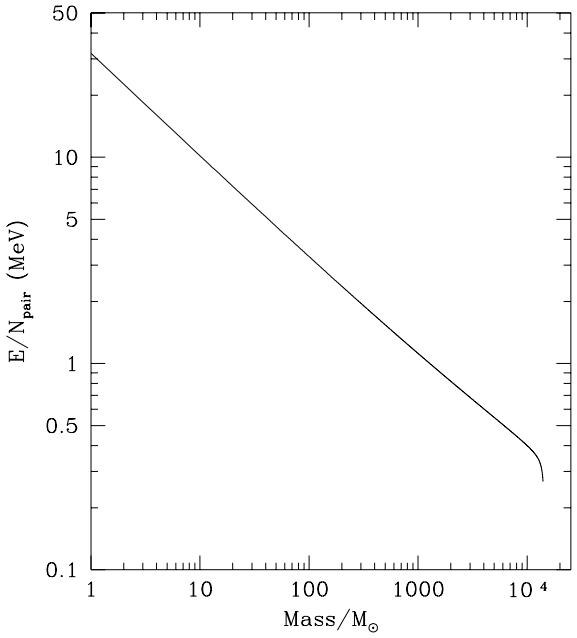

Fig. 2. An average energy per pair versus mass is given for a black hole with mass M and charge equal to 10% of maximal black hole charge: $\xi = 0.1$.

3. General relativistic hydrodynamic equations

In order to model the radial evolution of the e^+e^--pair and photon plasma fluid created in the dyadosphere of an EMBH, we need to discuss the relativistic hydrodynamic equations governing such an evolution and the associated rate equation for the pairs.

The metric for a Reissner-Nordstrom black hole is

$$ds^2 = -g_{tt}(r)dt^2 + g_{rr}(r)dr^2 + r^2 d\theta^2 + r^2 \sin^2\theta d\phi^2 \ , \quad (11)$$

where $g_{tt}(r) = -\left[1 - \frac{2GM}{c^2 r} + \frac{Q^2 G}{c^4 r^2}\right] \equiv -\alpha(r)^2$ and $g_{rr}(r) = \alpha(r)^{-2}$.

The plasma fluid of e^+e^--pairs, photons and baryon matter in the curved spacetime given by Eq. (11) is described by the covariant stress-energy tensor given by (Weinberg 1972)

$$T^{\mu\nu} = pg^{\mu\nu} + (p+\rho)U^\mu U^\nu + \Delta T^{\mu\nu}, \quad (12)$$

where ρ and p are respectively the total proper energy density and pressure in the comoving frame. U^μ is the four-velocity of the plasma fluid. $\Delta T^{\mu\nu}$ accounts for dissipative effects due to heat conduction, shear and bulk viscosity. In this paper, as a first approximation, we assume the plasma fluid of e^+e^- pairs, photons and baryon matter to be a simple perfect fluid in curved spacetime and neglect the dissipative terms $\Delta T^{\mu\nu}$ in Eq. (12). In spherical symmetry we have

$$g_{tt}(U^t)^2 + g_{rr}(U^r)^2 = -1 \ , \quad (13)$$

where U^r and U^t are the radial and temporal contravariant components of the 4-velocity. The conservation law for the baryon number can be expressed as a function of the proper baryon number density n_B as follows

$$\begin{aligned}(n_B U^\mu)_{;\mu} &= g^{-\frac{1}{2}}(g^{\frac{1}{2}} n_B U^\nu)_{,\nu} \\ &= (n_B U^t)_{,t} + \frac{1}{r^2}(r^2 n_B U^r)_{,r} = 0 \ . \end{aligned} \quad (14)$$

The energy-momentum conservation law of the plasma fluid is

$$\begin{aligned}(T^\sigma_\mu)_{;\sigma} &= \frac{\partial p}{\partial x^\mu} + g^{-\frac{1}{2}}\frac{\partial}{\partial x^\nu}\left[g^{\frac{1}{2}}(p+\rho)U_\mu U^\nu\right] \\ &+ \frac{1}{2}\frac{\partial g_{\nu\lambda}}{\partial x^\mu}(p+\rho)U^\nu U^\lambda = 0 \ . \end{aligned} \quad (15)$$

The radial component reduces to

$$\begin{aligned}&\frac{\partial p}{\partial r} + \frac{\partial}{\partial t}\left[(p+\rho)U^t U_r\right] + \frac{1}{r^2}\frac{\partial}{\partial r}\left[r^2(p+\rho)U^r U_r\right] \\ &- \frac{1}{2}(p+\rho)\left[\frac{\partial g_{tt}}{\partial r}(U^t)^2 + \frac{\partial g_{rr}}{\partial r}(U^r)^2\right] = 0 \ . \end{aligned} \quad (16)$$

The component of the energy-momentum conservation equation (15) along a flow line is

$$\begin{aligned}U_\mu (T^{\mu\nu})_{;\nu} &= -(\rho U^\nu)_{;\nu} - pU^\nu_{;\nu} \\ &= -g^{-\frac{1}{2}}(g^{\frac{1}{2}}\rho U^\nu)_{,\nu} - pg^{-\frac{1}{2}}(g^{\frac{1}{2}}U^\nu)_{,\nu} \\ &= (\rho U^t)_{,t} + \frac{1}{r^2}(r^2 \rho U^r)_{,r} \\ &+ p\left[(U^t)_{,t} + \frac{1}{r^2}(r^2 U^r)_{,r}\right] = 0 \ . \end{aligned} \quad (17)$$

Defining the total proper internal energy density ϵ and the baryon mass density ρ_B in the comoving frame

$$\epsilon \equiv \rho - \rho_B, \qquad \rho_B \equiv n_B m_B c^2 \ , \quad (18)$$

and using the law of baryon-number conservation (14), from Eq. (17) we have

$$(\epsilon U^\nu)_{;\nu} + pU^\nu_{;\nu} = 0\ . \tag{19}$$

Recalling that $\frac{dV}{d\tau} = VU^\mu_{;\mu}$, where V is the comoving volume and τ is the proper time for the fluid, we have along each flow line

$$\frac{d(V\epsilon)}{d\tau} + p\frac{dV}{d\tau} = \frac{dE}{d\tau} + p\frac{dV}{d\tau} = 0\ , \tag{20}$$

where $E = V\epsilon$ is total proper internal energy of the plasma fluid.

Finally, we represent the equation of state by a thermal index $\Gamma(\rho, T)$

$$\Gamma = 1 + \frac{p}{\epsilon}\ . \tag{21}$$

We now turn to the analysis of e^+e^- pairs initially created in the dyadosphere. Let n_{e^-} and n_{e^+} be the proper densities of electrons and positrons. We have

$$n_{e^-} = n_{e^+} = n_{\rm p}\ . \tag{22}$$

The rate equation for electrons and positrons gives

$$\begin{aligned}(n_{e^\pm}U^\mu)_{;\mu} &= (n_{e^\pm}U^t)_{,t} + \frac{1}{r^2}(r^2 n_{e^\pm}U^r)_{,r} \\ &= \overline{\sigma v}\left[n_{e^-}(T)n_{e^+}(T) - n_{e^-}n_{e^+}\right]\ ,\end{aligned} \tag{23}$$

where σ is the mean pair annihilation-creation cross-section, v is the thermal velocity of $e^\pm$, $\overline{\sigma v}$ is the average value of σv and $n_{e^\pm}(T)$ are the proper number-densities of electrons and positrons that thermalize with photons through the process $e^+e^- \leftrightarrow \gamma + \gamma$, $n_{e^\pm}(T) = n_\gamma(T)$ for $T > m_e c^2$, where $n_\gamma(T)$ is the number-density of photons. The proper number-densities $n_{e^\pm}(T)$ are given by appropriate Fermi integrals with zero chemical potential, at the equilibrium temperature T. The equilibrium temperature T is determined by the thermalization processes occurring in the PEM-pulse with a total proper energy-density ρ, whose evolution is governed by the hydrodynamic Eqs. (14,16,17). We have

$$\rho = \rho_\gamma + \rho_{e^+} + \rho_{e^-} + \rho^b_{e^-} + \rho_B, \tag{24}$$

where $\rho_\gamma = aT^4$ is the photon energy-density and $\rho^b_{e^-}$ is the energy-density of the electrons stemming from the ionization of baryonic matter, which is given by a Fermi integral with an appropriate chemical potential μ_e at the equilibrium temperature T, and $\rho_B \simeq m_B c^2 n_B$, where n_B is the baryon number-density, since baryons and ions are expected to be non-relativistic in the range of temperature T under consideration. $\rho_{e^\pm}$ is the proper energy-density of electrons and positrons of pairs defined by

$$\rho_{e^\pm} \equiv \frac{n_{e^\pm}}{n_{e^\pm}(T)}\rho_{e^\pm}(T), \tag{25}$$

where $n_{e^\pm}$ is obtained by integration of Eq. (23) and $\rho_{e^\pm}(T)$ is the proper energy-density of electrons (positrons) obtained from zero chemical potential Fermi integrals at the equilibrium temperature T. Having implicitly defined the equilibrium temperature T by Eq. (24), we can also analogously evaluate the total pressure

$$p = p_\gamma + p_{e^+} + p_{e^-} + p^b_{e^-} + p_B, \tag{26}$$

where p_γ is the photon pressure, $p_{e^\pm}$ defined by

$$p_{e^\pm} \equiv \frac{n_{e^\pm}}{n_{e^\pm}(T)}p_{e^\pm}(T), \tag{27}$$

where the pressures $p_{e^\pm}(T)$ are determined by zero chemical potential Fermi-integrals at the equilibrium temperature T, and $p^b_{e^-}$ is the pressure of the ionized electrons, evaluated by an appropriate Fermi integral of non-zero chemical potential μ_e. In Eq. (26), the ion pressure p_B is negligible by comparison with the pressures $p_{\gamma,e^\pm,e^-_b}(T)$. Finally, using Eqs. (24,26), we compute the thermal index Γ of the equation of state (21).

It is clear that in order to be correct, the entire set of equations considered above, namely Eqs. (14,16,17) with equation of state given by Eq. (21) and the rate equation (23) have to be integrated fulfilling the total energy conservation for the system. The boundary conditions adopted here are simply purely ingoing conditions at the horizon and outgoing at radial infinity.

The calculation is initiated by depositing a proper energy density (7) between the Reissner-Nordstrom horizon radius r_+ and the dyadosphere radius r_{ds}. The total energy deposited is given by Eq. (8). The calculation is continued as the plasma fluid expands, cools and the e^+e^- pairs recombine, until it becomes optically thin:

$$\int_R dr(n_{e^\pm} + \bar{Z}n_B)\sigma_T \simeq O(1), \tag{28}$$

where $\sigma_T = 0.665 \times 10^{-24}{\rm cm}^2$ is the Thomson cross-section is, $\bar{Z}$ is the average atomic number of baryon matter and the integration is over the radial interval of the PEM-pulse in the comoving frame. At this point the energy is virtually entirely in the form of free-streaming photons and the calculation is stopped. In the following computations we shall assume that baryonic matter is absent. The case of presence of baryonic matter, left over in a remnant during the process of gravitational collapse, is discussed in Ruffini et al., 1999 paper in preparation.

4. Numerical integration of general relativistic hydrodynamic equations

We use a computer code (Wilson et al. 1997, 1998) to evolve the spherically symmetric hydrodynamic equations for the baryons, e^+e^--pairs and photons deposited in the dyadosphere.

We define the generalized Lorentz factor γ and the radial coordinate velocity V^r

$$\gamma \equiv \sqrt{1 + U^r U_r}, \qquad V^r \equiv \frac{U^r}{U^t}. \tag{29}$$

From Eqs. (11, 13), we then have

$$(U^t)^2 = -\frac{1}{g_{tt}}(1 + g_{rr}(U^r)^2) = \frac{1}{\alpha^2}\gamma^2. \tag{30}$$

Following Eq. (18), we also define

$$E \equiv \epsilon\gamma, \quad D \equiv \rho_B\gamma, \quad \text{and} \quad \tilde{\rho} \equiv \rho\gamma \tag{31}$$

so that the conservation law of baryon number (14) can then be written as

$$\frac{\partial D}{\partial t} = -\frac{\alpha}{r^2}\frac{\partial}{\partial r}(\frac{r^2}{\alpha}DV^r). \tag{32}$$

Consequently, Eq. (17) acquires the form,

$$\frac{\partial E}{\partial t} = -\frac{\alpha}{r^2}\frac{\partial}{\partial r}(\frac{r^2}{\alpha}EV^r) - p\left[\frac{\partial\gamma}{\partial t} + \frac{\alpha}{r^2}\frac{\partial}{\partial r}(\frac{r^2}{\alpha}\gamma V^r)\right]. \tag{33}$$

Defining the radial coordinate momentum density

$$S_r \equiv \alpha(p+\rho)U^tU_r = (D+\Gamma E)U_r, \tag{34}$$

we can express the radial component of the energy-momentum conservation law given in Eq. (16) by

$$\begin{aligned}\frac{\partial S_r}{\partial t} &= -\frac{\alpha}{r^2}\frac{\partial}{\partial r}(\frac{r^2}{\alpha}S_rV^r) - \alpha\frac{\partial p}{\partial r} \\ &- \frac{\alpha}{2}(p+\rho)\left[\frac{\partial g_{tt}}{\partial r}(U^t)^2 + \frac{\partial g_{rr}}{\partial r}(U^r)^2\right] \\ &= -\frac{\alpha}{r^2}\frac{\partial}{\partial r}(\frac{r^2}{\alpha}S_rV^r) - \alpha\frac{\partial p}{\partial r} \\ &- \alpha\left(\frac{M}{r^2} - \frac{Q^2}{r^3}\right)\left(\frac{D+\Gamma E}{\gamma}\right)\left[\left(\frac{\gamma}{\alpha}\right)^2 + \frac{(U^r)^2}{\alpha^4}\right]. \end{aligned} \tag{35}$$

In order to determine the number-density of e^+e^- pairs, we turn to Eq. (23). Defining the e^+e^--pair coordinate density $N_{e^\pm} \equiv \gamma n_{e^\pm}$ and $N_{e^\pm}(T) \equiv \gamma n_{e^\pm}(T)$ and using Eq. (30), we rewrite the rate equation given by Eq. (23) in the form

$$\frac{\partial N_{e^\pm}}{\partial t} = -\frac{\alpha}{r^2}\frac{\partial}{\partial r}(\frac{r^2}{\alpha}N_{e^\pm}V^r) + \overline{\sigma v}(N^2_{e^\pm}(T) - N^2_{e^\pm})/\gamma^2, \tag{36}$$

where the equilibrium temperature T has been obtained from Eqs. (24) and (25).

5. A simple special relativistic treatment of the expansion of the PEM-pulse

In the following, using the definitions introduced in Sect. 4, we study the general properties of PEM-pulses. As the zeroth order approximation, we do not consider: (i) the gravitational interaction since it can be considered a perturbation against the total energy of the PEM-pulse and we describe the expanding fluid by a special relativistic set of equations, (ii) the radiation energy lost during expansion since this is a very small fraction of total energy before the dense PEM-pulse becomes transparent.

Analogous to Eq. (20), from Eq. (14), we have, in the general case of presence of baryonic matter, along each flow line,

$$\frac{d(n_BV)}{d\tau} = 0. \tag{37}$$

For a small shell of volume ΔV at radius r, for the expansion of that shell from the volume $\Delta V_\circ$ to the volume ΔV, we obtain

$$\frac{n_B^\circ}{n_B} = \frac{\Delta V}{\Delta V_\circ} = \frac{\Delta\mathcal{V}\gamma(r)}{\Delta\mathcal{V}_\circ\gamma_\circ(r)}, \tag{38}$$

where $\Delta\mathcal{V}$ is the volume of the shell in the coordinate frame and it relates to the proper volume ΔV in the comoving frame by $\Delta V = \gamma(r)\Delta\mathcal{V}$, where $\gamma(r)$ defined in Eq. (29) is the γ-factor of the shell at the radius r.

Similarly from Eq. (20), using the equation of state (21), along the flow lines we obtain

$$d\ln\epsilon + \Gamma d\ln V = 0. \tag{39}$$

With a very small variation of the volume from $\Delta V_\circ$ to ΔV and the internal energy density ϵ along the flow lines we obtain

$$\frac{\epsilon_\circ}{\epsilon} = \left(\frac{\Delta V}{\Delta V_\circ}\right)^\Gamma = \left(\frac{\Delta\mathcal{V}}{\Delta\mathcal{V}_\circ}\right)^\Gamma\left(\frac{\gamma(r)}{\gamma_\circ(r)}\right)^\Gamma, \tag{40}$$

where the thermal index Γ given by (21) is computed in for each value of ϵ, p as a function of ΔV. The thermal index Γ is a slowly-varying function of the state with values around $4/3$.

We know that as the PEM-pulse expands, the overall energy conservation requires that the change of total internal proper energy of a shell in the fluid will be compensated by a change in the bulk kinetic energy of the shell. We clearly have for the total internal proper energy of the PEM-pulse in the comoving frame

$$\mathcal{E}_{\Delta\mathcal{V}} = \int_{\Delta V}\rho dV = \int_{\Delta\mathcal{V}}\tilde{\rho}d\mathcal{V}, \tag{41}$$

where $dV(d\mathcal{V})$ is the proper (coordinate) volume of a fluid element in the shell of the PEM-pulse, and $\tilde{\rho}$ is defined by (31). The change of the kinetic energy of a fluid element in the shell of the PEM-pulse due to an infinitesimal expansion is given by,

$$dK = [\gamma(r) - 1](dE + \rho_B dV). \tag{42}$$

The total energy conservation for that shell implies

$$\mathcal{E}_{\Delta\mathcal{V}_\circ} - \mathcal{E}_{\Delta\mathcal{V}} = \int_{\Delta\mathcal{V}_\circ}\tilde{\rho}_\circ d\mathcal{V} - \int_{\Delta\mathcal{V}}\tilde{\rho}d\mathcal{V} = \int_{\Delta\mathcal{V}_\circ}^{\Delta\mathcal{V}} dK, \tag{43}$$

where $\mathcal{E}_{\Delta\mathcal{V}}$ is the total internal proper energy of the shell including baryon masses.

In order to model the relativistic expansion of plasma fluid analytically, we assume that E and D, as defined by Eq. (31), are constant in space over the volume ΔV. As a consequence, we can describe the system in terms of the relativistic Lorentz factor $\gamma(r)$, the volume $\Delta\mathcal{V}$ in coordinate frame and the quantities ϵ and ρ_B known in the comoving frame. We can rewrite the left-hand-side of Eq. (43) as

$$(\epsilon_\circ + \rho_B^\circ)\gamma_\circ(r)\Delta\mathcal{V}_\circ - (\epsilon + \rho_B)\gamma(r)\Delta\mathcal{V}, \tag{44}$$

and the right-hand-side of Eq. (43) as

$$(\epsilon+\rho_B)\Delta\mathcal{V}\gamma(r)(\gamma(r)-1) - (\epsilon_\circ+\rho_B^\circ)\Delta\mathcal{V}_\circ\gamma_\circ(r)(\gamma_\circ(r)-1). \tag{45}$$

Thus Eq. (43) simplifies to

$$(\epsilon_\circ + \rho_B^\circ)\gamma_\circ^2(r)\Delta\mathcal{V}_\circ = (\epsilon + \rho_B)\gamma^2(r)\Delta\mathcal{V}, \tag{46}$$

which leads the solution

$$\gamma(r) = \gamma_\circ(r)\sqrt{\frac{(\epsilon_\circ + \rho_B^\circ)\Delta\mathcal{V}_\circ}{(\epsilon + \rho_B)\Delta\mathcal{V}}}. \tag{47}$$

In the special relativistic case the rate equation (23) for $e^{\pm}$ reduces to

$$\frac{\partial(n_{e^\pm}\gamma(r))}{\partial t} = -\frac{1}{r^2}\frac{\partial}{\partial r}(r^2 n_{e^\pm}\gamma(r)V^r) + \overline{\sigma v}(n^2_{e^\pm}(T) - n^2_{e^\pm}). \quad (48)$$

In the shell of the PEM-pulse, we define the coordinate number-density of $e^{\pm}$ in equilibrium to be $N_{e^\pm}(T) \equiv \gamma(r)n_{e^\pm}(T)$ and correspondingly the coordinate number-density of $e^{\pm}$ to be $N_{e^\pm} \equiv \gamma(r)n_{e^\pm}$. With the assumption that $n_{e^\pm}$ in Eq. (23) is constant in space over the volume ΔV, we obtain the equation for the evolution of the $e^{\pm}$ coordinate number-density as they fall out of equilibrium with the PEM-pulse, as seen by a coordinate observer

$$\frac{\partial}{\partial t}(N_{e^\pm}) = -N_{e^\pm}\frac{1}{\Delta\mathcal{V}}\frac{\partial\Delta\mathcal{V}}{\partial t} + \overline{\sigma v}\frac{1}{\gamma^2(r)}(N^2_{e^\pm}(T) - N^2_{e^\pm}). \quad (49)$$

Eqs. (38), (40), (47) and (49) are a complete set of equations describing the relativistic expansion of the shell in the PEM-pulse.

If we now turn from a single shell of the PEM-pulse to a finite distribution of shells over the PEM-pulse, we introduce the average values of the proper internal-energy, baryon-mass, baryon-number and pair-number densities ($\bar{\epsilon}, \bar{\rho}_B, \bar{n}_B, \bar{n}_{e^\pm}$), and $\bar{E} \equiv \bar{\gamma}\bar{\epsilon}$, $\bar{D} \equiv \bar{\gamma}\bar{\rho}_B$, $\bar{N}_{e^\pm} \equiv \bar{\gamma}(r)\bar{n}_{e^\pm}$ for the PEM-pulse, where the average relativistic $\bar{\gamma}$-factor is defined by,

$$\bar{\gamma} = \frac{1}{\mathcal{V}}\int_{\mathcal{V}}\gamma(r)d\mathcal{V}, \quad (50)$$

and $\mathcal{V}$ is the total coordinate volume of the PEM-pulse. Considering the volume expansion of the PEM-pulse from $\mathcal{V}_\circ$ to $\mathcal{V}$, we transform Eqs. (38,40) into

$$\frac{\bar{n}^\circ_B}{\bar{n}_B} = \frac{V}{V_\circ} = \frac{\mathcal{V}\bar{\gamma}}{\mathcal{V}_\circ\bar{\gamma}_\circ}, \quad (51)$$

$$\frac{\bar{\epsilon}_\circ}{\bar{\epsilon}} = \left(\frac{V}{V_\circ}\right)^\Gamma = \left(\frac{\mathcal{V}}{\mathcal{V}_\circ}\right)^\Gamma\left(\frac{\bar{\gamma}}{\bar{\gamma}_\circ}\right)^\Gamma, \quad (52)$$

where $V = \bar{\gamma}\mathcal{V}$ is the total proper volume of the PEM-pulse, following from the definition $\bar{\gamma}$ in Eq. (50). Analogously, Eq. (46) becomes

$$(\bar{\epsilon}_\circ + \bar{\rho}^\circ_B)\bar{\gamma}^2_\circ\mathcal{V}_\circ = (\bar{\epsilon} + \bar{\rho}_B)\mathcal{V}\bar{\gamma}^2, \quad (53)$$

and Eq. (47) becomes

$$\bar{\gamma} = \bar{\gamma}_\circ\sqrt{\frac{(\bar{\epsilon}_\circ + \bar{\rho}^\circ_B)\mathcal{V}_\circ}{(\bar{\epsilon} + \bar{\rho}_B)\mathcal{V}}}, \quad (54)$$

while Eq. (49) becomes

$$\frac{\partial}{\partial t}(\bar{N}_{e^\pm}) = -\bar{N}_{e^\pm}\frac{1}{\mathcal{V}}\frac{\partial\mathcal{V}}{\partial t} + \overline{\sigma v}\frac{1}{\bar{\gamma}^2}(\bar{N}^2_{e^\pm}(T) - \bar{N}^2_{e^\pm}), \quad (55)$$

where the coordinate number-density of $e^{\pm}$-pairs in equilibrium is $\bar{N}_{e^\pm}(T) \equiv \bar{\gamma}n_{e^\pm}(T)$ and the coordinate number-density of $e^{\pm}$-pairs is $\bar{N}_{e^\pm} \equiv \bar{\gamma}\bar{n}_{e^\pm}$. For an infinitesimal expansion of the coordinate volume from $\mathcal{V}_\circ$ to $\mathcal{V}$ in the coordinate time interval $t - t_\circ$, we can discretize the differential Eq. (55) for numerical computations.

6. Three models of different geometry for the expansion of the PEM-pulse

We analyze three possible patterns of expansion of the PEM-pulse for those cases where the relationship between the average relativistic $\bar{\gamma}$ factor and the radial component of the four-velocity $U_r(r)$ is determined by the following respective conditions (see Eqs. (29,50))

– Spherical model: assuming the radial component of the four-velocity $U_r(r) = U\frac{r}{\mathcal{R}}$, where U is the radial component of the four-velocity at the moving outer surface ($r = \mathcal{R}(t)$) of the PEM-pulse, the $\bar{\gamma}$-factor and the velocity V_r are

$$\bar{\gamma} = \frac{3}{8U^3}\Big[2U(1+U^2)^{\frac{3}{2}} - U(1+U^2)^{\frac{1}{2}} - \ln(U + \sqrt{1+U^2})\Big], \quad V_r = \frac{U_r}{\bar{\gamma}}; \quad (56)$$

this distribution expands keeping an uniform density profile, decreasing with time, similar to a portion of a Friedmann Universe.

– Slab 1: assuming $U(r) = U_r = \text{const.}$, the constant width of the expanding slab $\mathcal{D} = R_\circ$ in the coordinate frame of the PEM-pulse, $\bar{\gamma}$ and V_r are

$$\bar{\gamma} = \sqrt{1+U^2_r}, \quad V_r = \frac{U_r}{\bar{\gamma}}; \quad (57)$$

this distribution does not need any averaging process.

– Slab 2: assuming a constant width $R_2 - R_1 = R_\circ$ of the expanding slab in the comoving frame of the PEM-pulse, $\bar{\gamma}$ and V_r are

$$\bar{\gamma} = \sqrt{1+U^2_r(\tilde{r})}, \quad V_r = \frac{U_r}{\bar{\gamma}}, \quad (58)$$

This distribution needs an averaging procedure and $R_1 < \tilde{r} < R_2$, i.e. $\tilde{r}$ is an intermediate radius in the slab.

In these three specific models of relativistic expansion, the average relativistic gamma factor $\bar{\gamma}$ is related differently to the radial component of the four-velocity $U(r)$ and the velocity of expansion. As a consequence, this leads to distinct relationships between the coordinate radius $\mathcal{R}$ and the coordinate time t in different models. This leads to the monotonically increasing $\bar{\gamma}$-factor as a function of the coordinate radius (or time) having a distinct slope (see Fig. 3). This slope varies from model to model. In principle, we could have an infinite number of models by defining the geometry of the expanding fluid. Thus, to find out which expanding pattern of PEM-pulses is the most physically realistic, we need to confront the results of our proposed theoretical simplified models with the numerical results based on the hydrodynamic Eqs. (32,33,35) and see if any one of them is in agreement with these results.

Eqs. (51,52,54,55) can be used to make numerical integrations to relate the quantities $\bar{\gamma}$,$\bar{\epsilon}$, $\bar{\rho}_B$ and $\bar{N}_{e^\pm}$ to $\bar{\gamma}_\circ$, $\bar{\epsilon}_\circ$, $\bar{\rho}^\circ_B$ and $\bar{N}^\circ_{e^\pm}$ in terms of the ratio $\frac{\mathcal{V}_\circ}{\mathcal{V}}$. We can consider each step of the adiabatic process of expansion from volume $\mathcal{V}_\circ$ to volume $\mathcal{V}$ to be infinitesimal. Given initial values of the quantities

$\bar{\gamma}_\circ, \bar{\epsilon}_\circ, \bar{\rho}^\circ_B$ and $\bar{N}^\circ_{e^\pm}$ in the volume $\mathcal{V}_\circ$ and temperature $T_\circ$ as well as $\bar{N}^\circ_{e^\pm}(T_\circ)$, we can obtain the values of $\bar{\gamma}$, $\bar{\epsilon}$ and $\bar{\rho}_B$ corresponding to the volume $\mathcal{V}$ by using computer to solve these three dynamical Eqs. (51,52,54). With the value of $\bar{\gamma}$ obtained we find the corresponding velocity V_r by Eqs. (29,56,57,58) and the coordinate time $t = t_\circ + \Delta t, \Delta t = \Delta\mathcal{R}/V_r$, where $t_\circ, t$ are the times corresponding to expanding volumes $\mathcal{V}_\circ, \mathcal{V}$ respectively and $\mathcal{R} = \mathcal{R}_\circ + \Delta\mathcal{R}$, where $\delta\mathcal{R}$ is the variation of the coordinate radius at the surface of the PEM-pulse as its volume changes from volume $\mathcal{V}_\circ$ to volume $\mathcal{V}$. Then we find the corresponding number of pairs $\bar{N}_{e^\pm}$ by solving the rate equation (55). Next we evaluate the fraction $\frac{\bar{N}_{e^\pm}}{\bar{N}_{e^\pm}(T_\circ)}$ and the appropriate Fermi integrals in the right-hand-side of Eqs. (24,25), so that we can determine the temperature T of the equilibrium state corresponding to the volume $\mathcal{V}$ from the proper energy-density through Eqs. (24,25). Then by iterative computing steps, $\mathcal{V}_\circ, \mathcal{V}_1, \mathcal{V}_2, \cdots$, we can describe the whole process of the expanding PEM-pulse. As a result, given initial values $\bar{\gamma} = 1, \mathcal{R}_\circ = r_{ds}$, $T_\circ$, $\bar{\rho}^\circ_B$, $\bar{\epsilon}_\circ$ and $\bar{N}_{e^\pm} = \bar{N}_{e^\pm}(T_\circ)$ of a dyadosphere discussed in Sect. 1, we can obtain $\bar{\gamma}(\mathcal{R})$ and energy-density $\bar{\epsilon}(\mathcal{R})$ of the expanding PEM-pulse in terms of the coordinate radius $\mathcal{R}$ and time t. The calculations are continued until the plasma becomes optically thin as expressed by the condition (28). In fact, Eqs. (53,54) are equivalent to

$$\frac{d(\bar{\rho}\bar{\gamma}^2\mathcal{V})}{dt} = 0, \tag{59}$$

the conservation of the total energy of the PEM-pulse at each expanding step, and we check that it is fulfilled at each numerical iteration step.

From the conservation of entropy it follows that asymptotically we have

$$\frac{(VT^3)_{T<mc^2}}{(VT^3)_{T>mc^2}} = \frac{11}{4}\,, \tag{60}$$

exactly for the same reasons and physics scenario discussed in the cosmological framework by Weinberg, see e.g. Eq. (15.6.37) of Weinberg (1972): the present equation follows by substituting the comoving volume factor R^3 by the comoving volume V in the cited equation. The same considerations when repeated for the conservation of the total energy $\bar{\rho}\bar{\gamma}V = \bar{\rho}\bar{\gamma}^2\mathcal{V}$ following from Eq. (59) then lead to

$$\frac{(VT^4\bar{\gamma})_{T<mc^2}}{(VT^4\bar{\gamma})_{T>mc^2}} = \frac{11}{4}\,. \tag{61}$$

The ratio of these last two relations then gives asymptotically

$$T_\circ = (T\bar{\gamma})_{T>mc^2} = (T\bar{\gamma})_{T<mc^2}, \tag{62}$$

where $T_\circ$ is the initial average temperature of the dyadosphere at rest, given in Fig. 2. Eq. (62) explains the approximate constancy of $T\bar{\gamma}$ shown in Fig. 7.

7. Analysis of the spectrum and lightcurve at the time of decoupling

We are interested in the observed spectrum at the time of decoupling. To calculate the spectrum, we assume that (i) the plasma fluid of coupled e^+e^- pairs and photons undergoes adiabatic expansion and does not emit radiative energy before they decouple (this assumption is relaxed in Preparata & Ruffini, 1999 and Preparata et al., 1999 (papers in preparation); (ii) the e^+e^- pairs and photons are in equilibrium at the same temperature T when they decouple. Thus the photons in the fluid frame (de-

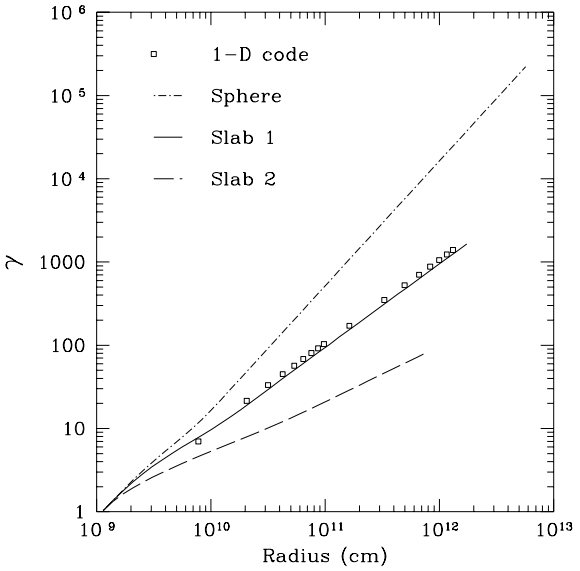

Fig. 3. Lorentz gamma factor γ as a function of radius. Three models for the expansion pattern of the PEM-pulse are compared with the results of the one dimensional hydrodynamic code for a $1000M_\odot$ black hole with charge to mass ratio $\xi = 0.1$. The 1-D code has an expansion pattern that strongly resembles that of a shell with constant coordinate thickness.

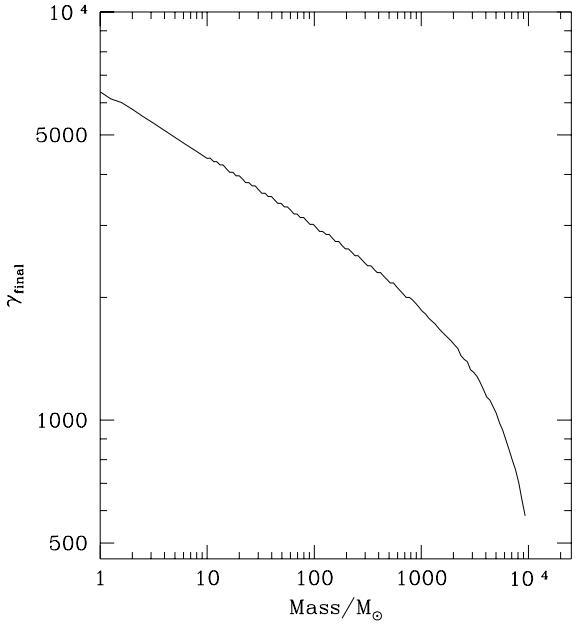

Fig. 4. In the expansion model of a shell with constant coordinate thickness, the decoupling gamma-factor $\gamma_{\rm final}$ as a function of EMBH masses is plotted with charge to mass ratio $\xi = 0.1$.

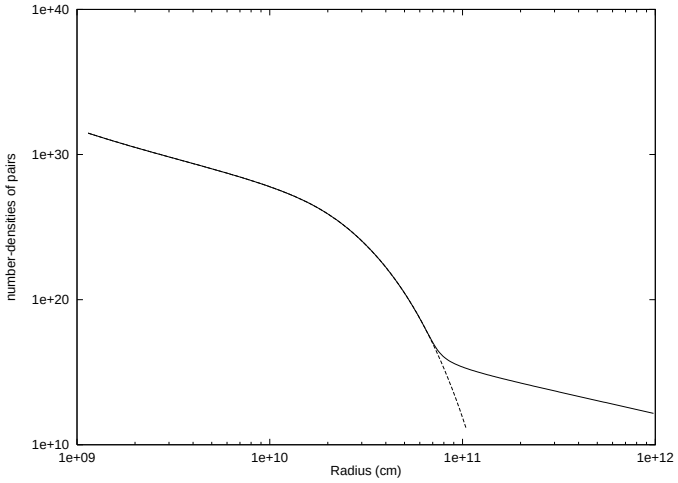

Fig. 5. The number-densities ($N_{e^\pm}/\mathrm{cm}^{-3}$) of pairs $n_{e^\pm}$ (solid line) as obtained from the rate equation (23), and $n_{e^\pm}(T)$ (dashed line) as computed by Fermi-integrals with zero chemical potential, provided the temperature T determined by the equilibrium condition (24), are plotted for a $1000M_\odot$ black hole with charge to mass ratio $\xi = 0.1$. For $T < m_e c^2$, the two curves strongly diverge.

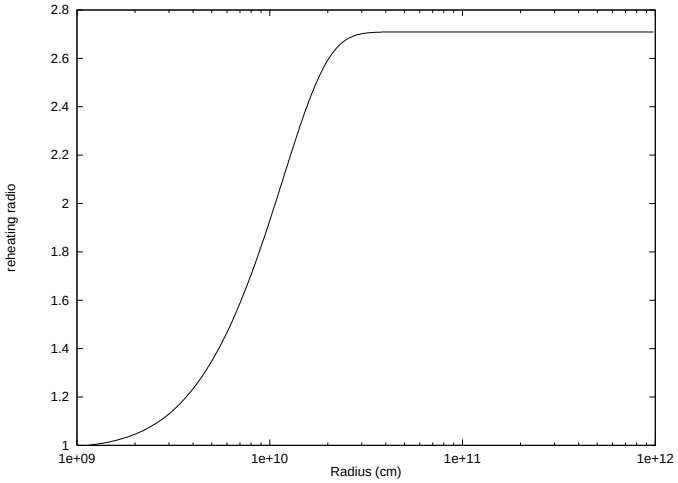

Fig. 6. The reheating ratio $T^3V/T_\circ^3V_\circ$ defined by Eq. (60) is plotted as a function of radius for a $1000M_\odot$ black hole with charge to mass ratio $\xi = 0.1$. The rate equation (23) with definition (25) naturally leads to the value $\frac{11}{4}$ after e^+e^--annihilation has occurred.

noted with a prime: $'$) are described by a Planck distribution of the form

$$u'_{\epsilon'}(T') \approx \frac{\epsilon'^3}{exp(\frac{\epsilon'}{T'}) - 1}, \tag{63}$$

where T' is the local temperature in the fluid frame of one thin shell. However, u_ϵ/ϵ^3 is a relativistic invariant resulting from the Liouville theorem (see e.g. Ehlers 1971). This implies ϵ/T is also a relativistic invariant. So a Planck distribution in an emitter's rest-frame with temperature T' will appear Planckian to a moving observer, but with boosted temperature $T = T'/(\gamma(1 - \frac{v}{c}\cos\theta))$ where $\frac{v}{c}\cos\theta$ is the component of fluid velocity directed toward the observer. Thus

$$u_\epsilon(\theta, v, T') \approx \frac{\epsilon^3}{exp(\gamma(1 - \frac{v}{c}\cos\theta)\frac{\epsilon}{T'}) - 1} \tag{64}$$

gives the observed spectrum of a blackbody with fluid-frame temperature T' moving at velocity v and angle θ with respect to the observer.

We wish to calculate the spectrum from a spherical, relativistically expanding shell as seen by a distant observer. We know the velocity v and proper temperature T' and shell radius R, so we integrate over volume and angle with respect to the observer. We thus get the observed number spectrum N_ϵ, per photon energy ϵ, per steradian, of a relativistically expanding spherical shell with radius R, thickness dR in cm, velocity v, Lorentz factor γ and fluid-frame temperature T' to be (in photons/eV/4π)

$$N_\epsilon(v, T', R) \equiv \int dV \frac{u_\epsilon}{\epsilon} = (5.23 \times 10^{11}) 4\pi R^2 dR \frac{\epsilon T'}{v\gamma} \cdot \log\left[\frac{1 - exp[-\gamma\epsilon(1 + \frac{v}{c})/T']}{1 - exp[-\gamma\epsilon(1 - \frac{v}{c})/T']}\right], \tag{65}$$

which has a maximum at $\epsilon_{max} \cong 1.39\gamma T'\ eV$ for $\gamma \gg 1$. We may then sum this spectrum over all shells (the zones in our computer code) of our PEM-pulse to get the total spectrum. Since we had assumed the photons are thermal in the comoving frame, our spectrum has now an high frequency exponential tail, and the spectrum appear as not thermal. In Fig. 8 we see the observed number spectral peak energy as a function of the EMBH mass with charge to mass ratio $\xi = 0.1$.

To obtain the observed light curve $\varepsilon(t)$ we again decompose the spherical PEM-pulse into concentric shells and consider two effects. First is the relative arrival time of the first light from each shell: light from outer shells will be observed before light from inner shells. Second is the shape of the light curve from a single shell.

Emission from the moving PEM-pulse is beamed along the direction of travel within an angle $\theta \sim 1/\gamma$. The surface of simultaneity of a relativistically expanding spherical shell as seen by an observer is an ellipsoid (see e.g. Fenimore et al. 1996). The time of intersection of an expanding ellipse and a fixed shell of radius R as a function of θ (i.e. the time at which emission from this intersection circle is received) is

$$t = \frac{R}{v}(1 - \frac{v}{c}\cos\theta) = (1 - \cos\theta)R + \frac{R}{v}(1 - \frac{v}{c})\,. \tag{66}$$

We find that, integrating our boosted Planck distribution of photons Eq. (64) over frequency, a relativistically expanding shell of radius R and thickness dR will have a time profile (in ergs/second/4π)

$$\varepsilon(\tau, v, T', R) = \frac{a}{2}\left(\frac{T'}{\tau}\right)^4 \frac{cR^2 dR}{v\gamma^4} \tag{67}$$

for $(1 - \frac{v}{c}) \leq \tau \leq (1 + \frac{v}{c})$, where $\tau \equiv \frac{vt}{R}$ and a is the radiation constant. Thus the larger the radius R of the expanding shell at

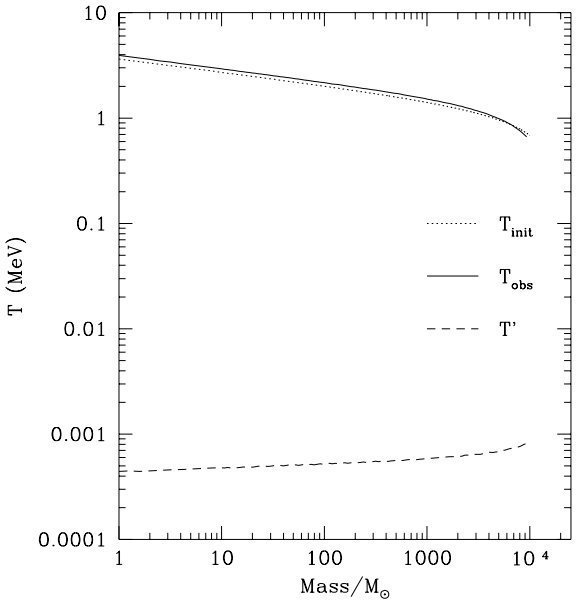

Fig. 7. Temperature of the plasma is shown over a range of masses. $T_{\rm init}$ is the average initial temperature of the plasma deposited around the EMBH, $T_{\rm obs} = 1.39\gamma_{\rm final}T'$ is the observed temperature of the plasma at decoupling while T' is the comoving temperature at decoupling. Notice that $\gamma T' \simeq T_{\rm init}$ as expected from Eq. (62).

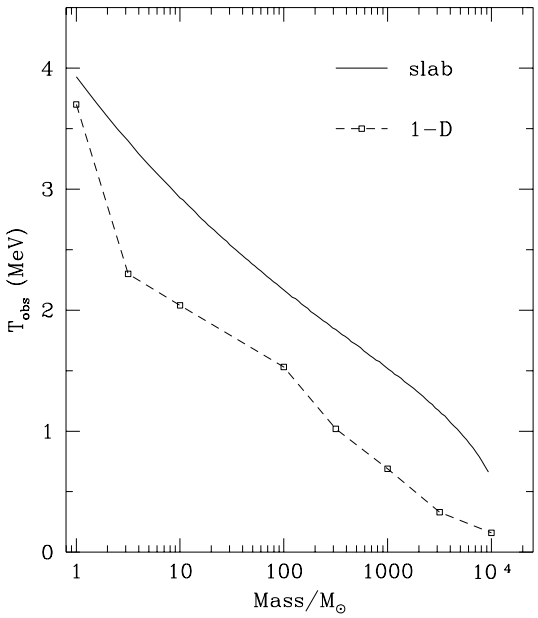

Fig. 8. The peak of the observed number spectrum as a function of the EMBH mass is plotted with charge to mass ratio $\xi = 0.1$. The observed peak temperature $T_{\rm obs}$ of the number spectrum is calculated from Eq. (65). The temperature for the slab of constant coordinate thickness is given by $T_{\rm obs} = 1.39\gamma_{\rm final}T'$; the peak of Eq. (65).

the moment of emission, the broader the $1/\tau^4$ tail on the light curve. The final light curve is then constructed by summing the signal from all shells.

A useful quantity which may be compared with observations is t_{90}; the time over which 90% of the emission is received. The

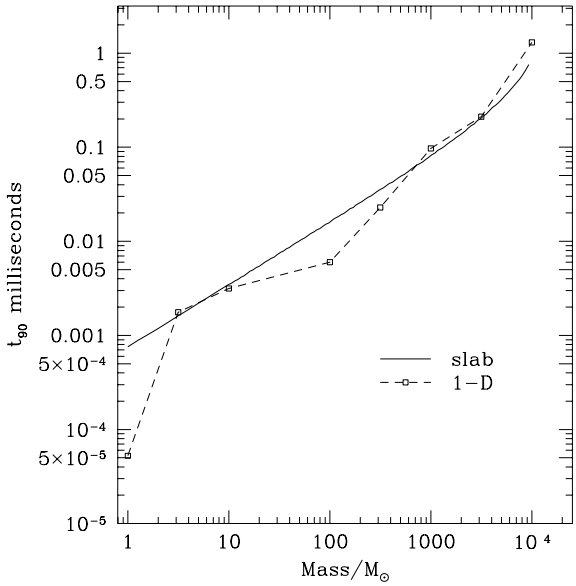

Fig. 9. The duration of the emission at decoupling is represented by t_{90}, the time over which 90% of the emission is received, plotted over a range of black hole masses. The 1-D hydrodynamic t_{90} is calculated from Eq. (67) and the slab t_{90} is calculated from Eq. (69). Note that the 1-D and slab models deviate for black hole mass $M = 1M_{\odot}$. This is because the energy density Eq. (7) deposited in the 1-D computations is not well approximated by a constant over the volume as in the slab model for small black hole mass.

t_{90} duration for a single shell can be calculated in the relativistic limit ($\gamma \gg 1$) by defining $\varepsilon(\tau) \equiv \varepsilon_0 \tau^{-4}$ and setting

$$\int_{1-\frac{v}{c}}^{1-\frac{v}{c}+\tau_{90}} \varepsilon(\tau)d\tau = 0.9 \int_{1-\frac{v}{c}}^{1+\frac{v}{c}} \varepsilon(\tau)d\tau, \tag{68}$$

which gives $\tau_{90} \approx 4.3/\gamma^2$. So the emission duration in seconds is

$$t_{90} \approx \tau_{90}\frac{R}{c} = 4.3\frac{R}{\gamma^2 c} \tag{69}$$

for $\gamma \gg 1$. Burst durations are shown in Fig. 9 for a range of EMBH masses with charge to mass ratio $\xi = 0.1$.

8. Results and discussion

Preliminary results have been presented in Ruffini (1999a), Ruffini et al.(1999a) and Ruffini (1999b). In the results presented here we consider a range of black hole masses from 1 to $10^4 M_{\odot}$ and we assume a charge of $Q = 0.1Q_{max}$ ($\xi = 0.1$). Over this mass range, and with this charge, a large amount of energy ($\sim 10^{52}$–10^{54} ergs) is available to be deposited within the dyadosphere, in the form of e^+e^- pairs, due to the process of vacuum polarization (Fig. 1). In Fig. 2 correspondingly the average energy of the created pairs are given as a function of the EMBH mass. These energies and spectral distributions are in the range of interest for gamma-ray bursts.

We have analyzed the evolution of this PEM pulse by a simple relativistic treatment in flat space for three different cases:

1) an expansion with a spatial component of the four velocity proportional to the distance, 2) an expansion with a width of the P EM pulse constant in the coordinate space and 3) an expansion with a width of the PEM pulse constant in the comoving frame. We have then compared and contrasted these results with the general relativistic hydrodynamic calculations. In Fig. 3 we see a comparison of the Lorentz factor of the expanding fluid as a function of radius for all of the models. We can see that the one-dimensional code matches the expansion pattern of a shell of constant coordinate thickness. The astrophysically unprecedented large Lorentz factors are reproduced in Fig. 4 as a function of the EMBH mass.

In Fig. 5 and Figs. 6,7 we describe the approach to transparency, as given by Eq. (28). In Fig. 5 we plot the number-densities of pairs $n_{e^\pm}$ given by the rate equation (23) and $n_{e^\pm}(T)$ computed from a Fermi-integral with zero chemical potential with the temperature T determined by the equilibrium condition (24). It clearly indicates that the pairs $e^\pm$ fall out of equilibrium as the temperature drops below the threshold of $e^\pm$-pair annihilation. As a consequence of pair $e^\pm$-annihilation, the crossover of this reheating process is shown in Fig. 6. Fig. 7 illustrates the extreme relativistic nature of the PEM pulse expansion: at decoupling, the local comoving plasma temperature is < 1 keV, but is boosted by $\gamma_{\rm final}$ to ~ 1 MeV and its relation to the initial energy of the PEM pulse in the dyadosphere is presented.

The spectrum and light-curve of the emitted pulse of radiation are analyzed as described in Sect. 7. We see the results for both the hydrodynamic and slab calculations compared in Figs. [8] & [9]. The 1-D hydrodynamic code spectral peak and burst duration t_{90} are consistently somewhat lower than those of the slab calculations due to gravitational and hydrodynamical effects. The peak photon energy of the photon number spectrum is in the range of 100–1000 keV, which is consistent with observed gamma-ray bursts. The duration of the burst is characterized by the t_{90} time, the time taken to receive 90% of the radiation. Over the mass range analyzed, t_{90} is of order a millisecond. This is shorter than observed gamma-ray bursts ($\sim$ 1–10 seconds, see e.g. Tavani 1998), but the collision of the PEM pulse with the remnant left over by the process of gravitational collapse produces longer emission times, see e.g. Ruffini et al., 1999; Preparata & Ruffini, 1999; Preparata et al., 1999 papers in preparation.

We have demonstrated that the concept of an EMBH in vacuum can produce a gamma-ray burst having many of the general characteristics of observed bursts validating the scenario presented in Ruffini 1998. This simplified model merits further detailed study of the collapse of highly magnetized stars in galaxies ($M \sim 10 M_\odot$) and gravitational collapse process occurring in galactic nuclei ($M \sim 10^4$–$10^5 M_\odot$). In particular, it is important to identify how, during the process of gravitational collapse to an EMBH, the breakdown of the magneto-hydrodynamic conditions leads to the formation of the dyadosphere. Future work will explore some additional important aspects of the PEM pulse including (i) the presence of baryonic matter left in the remnant around the EMBH during the process of gravitational collapse and its effect on the relativistic expansion (Ruffini et al., 1999 paper in preparation), (ii) the radiation emitted prior to decoupling and its effect on the dynamics of the PEM pulse in Preparata & Ruffini, 1999 and Preparata et al., 1999 papers in preparation, and (iii) the emission in the latest stages of evolution of the PEM pulse and its comparison with the observed bursts and afterglows in Preparata & Ruffini, 1999 and Preparata et al., 1999 papers in preparation.

Acknowledgements. J. D. Salmonson and J. R. Wilson were supported under the auspices of the U.S. Department of Energy by the Lawrence Livermore National Laboratory under contract W-7405-ENG-48. J.R. Wilson has additional support from NSF grant No. PHY-9401636. It is a pleasure to thank the referee and R. Jantzen for helpful suggestions in the wording of the manuscript.

References

Baring M.G., Harding A.K., 1998, ApJ 507, L55
Bloom J.S., Odewahn S.C., Djorgovski S.G., et al., 1999, ApJ 518, L1
Christodoulou D., Ruffini R., 1971, Phys. Rev. D4, 3552
Damour T., Ruffini R., 1975, Phys. Rev. Lett. 35, 463
Damour T., Hanni R.S., Ruffini R., Wilson J.R., 1978, Phys. Rev. D17, 1518
Ehlers J., 1971, In: Sachs R.K. (ed.) Proceedings of course 47 of the International School of Physics: Enrico Fermi, Academic Press, New York
Frontera F., Piro L., 1999, In: Frontera F., Piro L. (eds.) Proc. of Gamma-ray bursts in the afterglow era, Rome, Nov.3–6, 1998, to be published in A&AS
Fenimore E.E., Madras C., Nayakshin S., 1996, ApJ 473, 998
Heisenberg W., Euler H., 1931, Zeits. Phys. 69, 742
Kouveliotou C., Dieters S., Strohmayer T., et al., 1998, Nat 393, 35
Preparata G., Ruffini R., Xue S.-S., 1998a, submitted to Phys. Rev. Lett.
Preparata G., Ruffini R., Xue S.-S., 1998b, A&A 338, L87
Ruffini R., Wilson J.R., 1975, Phys. Rev. D12, 2959
Ruffini R., 1998, In: Sato H., Sugiyama N. (eds.) Black Holes and High Energy Astrophysics. Proceedings of the 49th Yamada Conference, Universal Ac. Press Tokyo
Ruffini R., 1999a, In: Piro L., Frontera F. (eds.) The dyadosphere of black holes and gamma-ray bursts. Proc. of Gamma-ray bursts in the afterglow era, Rome Nov.3–6, 1998, to be published in A&AS
Ruffini R., 1999b, The Dyadosphere of black holes and Gamma Ray Bursts. Proc. of 19th Texas Symposium, Paris, Dec. 1998
Ruffini R., Salmonson J., Wilson J.R., Xue S.-S., 1999a, In: Piro L., Frontera F. (eds.) On structure and temporal evolution of pair and electromagnetic pulse of an electromagnetic black hole. Proc. of Gamma-ray bursts in the afterglow era, Rome, Nov.3–6 1998, to be published in A&AS
Schwinger J., 1951, Phys. Rev. 82, 664
Tavani M., 1998, ApJ 497, L21
Weinberg S., 1972, Gravitation and Cosmology. John Wiley & Sons, Inc., USA
Wilson J.R., 1975, Annals of the New York Academy of Sciences 262, 123
Wilson J.R., 1977, In: Ruffini R. (ed.) Proc. of the First Marcel Grossmann Meeting on General Relativity. North-Holland Pub., Amsterdam, p. 393
Wilson J.R., Salmonson J.D., Mathews G.J., 1997, In: Meegan C.A., Preece R.D., Koshut T.M. (eds.) Gamma-Ray Bursts: 4th Huntsville Symposium, American Institute of Physics
Wilson J.R., Salmonson J.D., Mathews G.J., 1998, In: 2nd Oak Ridge Symposium on Atomic and Nuclear Astrophysics, IOP Publishing Ltd